

AD-A103 040

RENSSELAER POLYTECHNIC INST TROY NY DEPT OF MATERIAL--ETC F/G 11/6  
LIQUID AND SOLID METAL EMBRITTEMENT.(U)

N00014-79-C-0583

SEP 81 N S STOLOFF

NL

UNCLASSIFIED

TR-3

1 of 1  
280048


END  
DATE  
FILMED  
DTIC

AD A103048

(12)

14 TIK-3

(1) Technical Report, No. 3

to

Office of Naval Research

Contract N00014 - 79C9583

(13) November 1979

entitled

(6)

LIQUID AND SOLID METAL EMBRITTLEMENT.

Submitted by

(17) 32

(19) Norman M.S. Stoloff

Rensselaer Polytechnic Institute

Troy, New York 12181 U.S.A.

(11) 5 September 1981

DTIC ELECTED AUG 19 1981

A

Reproduction in whole or in part is permitted for any purpose of the United States Government. Distribution of this document is unlimited.

3 2 1 2


81 8 19 053  
21 8 10 053

DTIC FILE COPY

## LIQUID AND SOLID METAL EMBRITTLEMENT

Norman S. Stoloff

Materials Engineering Department  
Rensselaer Polytechnic Institute  
Troy, New York 12181



### INTRODUCTION

Low melting metals can interact with metallic substrates in several distinct ways that lead to premature fracture or surface degradation. The most spectacular, and widely studied, manifestation of metal-induced embrittlement (MIE) is the sudden fracture of stressed metals with little or no apparent inter-diffusion or chemical interaction. In this classical form of embrittlement, ductility is minimized at or near the melting point of the metallic surface film, and is then restored at some higher temperature, as shown in Fig. 1 for zinc embrittled by indium (1). Similar embrittlement may be noted when the surface film is solid, but the degree of embrittlement is reduced and then disappears as the temperature falls well below the melting point of the embrittler - 100°C or so in the case of lead on (or in) steel (2). Other manifestations of liquid metal embrittlement are connected with rapid penetration of the environment along grain boundaries (e.g. gallium on aluminum), by preferential chemical reactions (e.g. lithium on iron containing carbon or carbides), and by corrosion, perhaps aided by cavitation, in ferritic steel tubing containing mercury in a thermal gradient. In the latter case, failure of the component may occur either by thinning or ultimate penetration of the wall, or by mass transfer-caused plugging of the tube. In several instances, two or more of these phenomena may appear either simultaneously or under different exposure conditions with the same combination of environment and substrate, for example, aluminum single crystals and polycrystals also may suffer "instantaneous" embrittlement due to gallium.

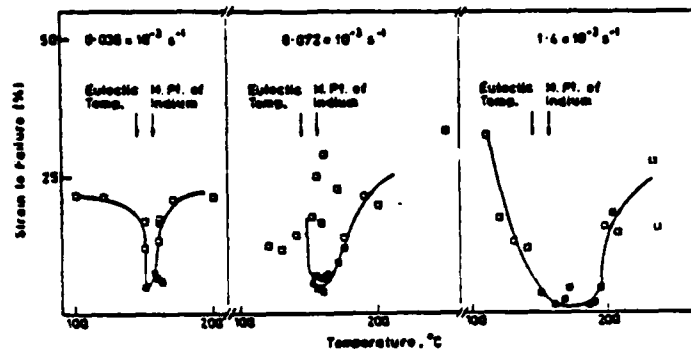


Fig. 1. Effect of temperature on tensile ductility of zinc tested in indium at various strain rates (1).

Shchukin et al (3) have reported that molten metals may also reduce fracture strength of covalently bonded materials, e.g. germanium is embrittled by gold and gallium and graphite by alkali metals. Low melting metals also reportedly reduce the strength of  $Al_2O_3$ .

Practical implications of these various embrittlement or degradation phenomena may be noted in widely diverse industrial situations, e.g.:

- a) embrittlement of alloys containing low melting metallic inclusions, as in steels and aluminum alloys to which lead is added to improve machinability.
- b) deterioration of alkali metal piping system in nuclear fission or fusion devices relying upon liquid metal coolants, as in the liquid metal fast breeder reactor or in lithium-moderated fusion devices.
- c) embrittlement stemming from plating of structural parts, as in cadmium on steel or titanium alloys.
- d) welding, brazing, or soldering operations, as in steels where copper contamination (from welding electrodes) may occur, or solder contacting stressed iron-base alloys.
- e) various industrial situations where molten metals are handled or where metal coatings are heated above their melting points.

Although metal-induced embrittlement is usually to be avoided, workers in the Soviet Union have utilized liquid metals, such as Pb-Sn eutectics, to facilitate drilling steels, Ni-Cr heat resistant alloys, titanium alloys, and others (3,4). Improvement achieved with liquid metals included increased drill life and improvement of the quality of machined surfaces.

From a scientific point of view, catastrophic failure without

apparent diffusion, i.e. classical liquid metal embrittlement, has received the most attention. The first portion of this paper is devoted to review of the principal features of this type of embrittlement, followed by an examination of the usefulness of various predictive criteria for identifying embrittlement couples and a critical evaluation of several proposed mechanisms of embrittlement. Emphasis will be on monotonic or static loading situations, since the literature of metal-induced embrittlement under cyclic loading has been reviewed recently (5). The balance of the paper will summarize the status of our understanding of alkali-metal induced embrittlement processes.

#### PREREQUISITES FOR EMBRITTLEMENT

It is generally accepted that for metal-induced embrittlement to occur, a stressed metal must be wetted by the liquid, the stress state should be one in which either primary or secondary tensile stresses are generated, and the temperature should be near that of the melting point of the embrittler. The precise relation between test temperature and the melting point cannot be predicted, since for many systems embrittlement occurs well below  $T_m$ : for example, embrittlement of AISI 4140 steel begins at  $T/T_m = 0.75$  for cadmium, and 0.85 for lead and tin environments (2). In a few cases, e.g. zinc embrittled by tin, the lower limiting temperature for embrittlement is  $T_E$ , the melting point of the eutectic between substrate and embrittler (1). In other cases, e.g. Zn-Hg and Zn-Ga (1), there is no embrittlement reported at any temperature below  $T_m$ , and in fact embrittlement may only be observed at  $T > T_m$ , as in the embrittlement of austenitic stainless steel by zinc (6) or pure iron by indium (7); the width of the temperature range over which embrittlement occurs depends upon strain rate and can be over 300°C (brass-Hg) (8) or as little as 5°C (Zn-Sn), Fig. 1 (1). In addition to the basic conditions for embrittlement set forward above (wetting of the substrate, tensile stresses, correct temperature range), the degree of embrittlement depends upon other conditions, such as grain size of the substrate or imposed strain rate. Therefore, the number of combinations of environment and substrate that are found to be embrittlement couples is constantly expanding, as wider variations in test conditions are imposed. Among the "new" embrittlement couples recently reported have been Zn-In (1), Al-Bi (9) and Al-Pb (9). Data for the latter systems appear in Fig. 2. This work, in which aluminum alloys containing inclusions of bismuth, cadmium or lead were tested in impact, showed that maximum embrittlement required at least 0.2% of either solute, suggesting that sufficient embrittler must be present to facilitate propagation as well as nucleation of a crack. The original demonstration of this phenomenon involved blunting of gallium-initiated surface cracks in cadmium with intentionally small amounts of liquid placed on the surface (10). However, notch-sensitive substrates such as Fe-3.5%Si can be fractured with very small amounts of embrittler (11).

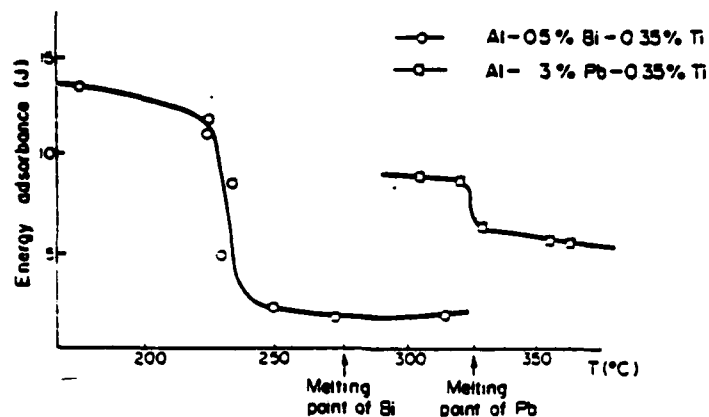


Fig. 2. Temperature dependence of energy absorbed during impact testing of aluminum containing bismuth or lead inclusions (9).

#### Metallurgical and Test Variables

The most widely utilized model for explaining the role of metallurgical variables in brittle fracture processes is the Cottrell (12)-Petch (13) relation, which was originally stated in the form:

$$\sigma_y k_s d \geq \beta \mu \gamma \quad (1)$$

where  $\sigma_y$  is yield stress,  $k_s$  is the slope of a (shear) yield stress vs.  $d^{-1/2}$  plot,  $d$  is one-half the grain diameter,  $\beta$  is a geometrical constant,  $\mu$  is the shear modulus and  $\gamma$  is the effective surface energy for fracture. This equation may also be rewritten as:

$$\sigma_1 k_s d^{1/2} + k_y k_s \geq \beta \mu \gamma \quad (2)$$

If yielding and fracture are viewed as competitive factors, ductile behavior is promoted by low yield stress, small grain size, and low resistance of grain boundaries to propagation of slip, while fracture is promoted by reduced shear modulus or surface energy. A ductile to brittle transition is predicted to occur in those materials, principally bcc metals, where  $\sigma_1$  is temperature dependent, since neither  $\mu$  nor  $\gamma$  is expected to vary appreciably with temperature.

It has been proposed that liquid metals reduce the energy associated with fracture, and perhaps the shear modulus at a crack tip as well, thereby inducing brittle fracture in ordinarily ductile metals and alloys (10). The precise nature of the surface energy lowering will be described later; for now it is only necessary to consider the consequences of a reduction in that energy, including

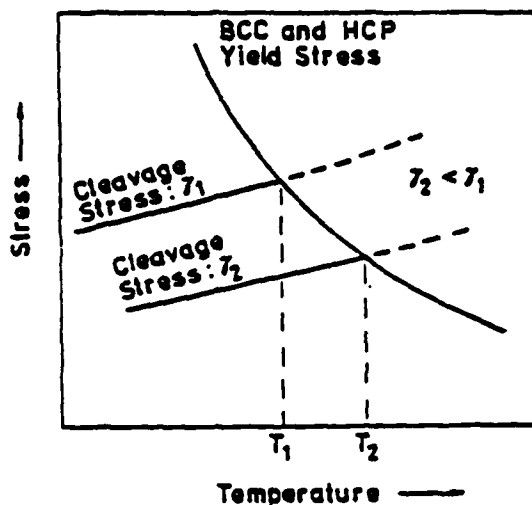


Fig. 3. Schematic diagram showing influence of surface energy on fracture stress and transition temperature (1).

any changes in the plastic work associated with crack propagation. Figure 3 shows schematically how a ductile to brittle transition can be obtained in bcc or hcp metals with temperature-dependent yield stresses, and nearly temperature independent fracture stresses (1, 14). Note that lowering the surface energy from  $\gamma_1$  to  $\gamma_2$ , as by testing in a liquid or solid metal environment, causes a significant increase in the transition temperature; no conclusion need be reached as to the precise mechanism of lowering of  $\gamma$ . In all cases, coarse grain size increases the likelihood of brittle fracture.

Equation (2) shows clearly that the transition to brittle fracture should be aided by any factor that raises  $\sigma_f$ . These would generally include decreasing temperature and increasing strain rate. Recently, there has been considerable attention directed to the effect of strain rate, as outlined below.

The ductile to brittle transition temperature of polycrystalline zinc tested in air ranges between  $-30^\circ\text{C}$  to  $+11^\circ\text{C}$ , dependent upon strain rate. Testing zinc in tin or indium environments at high strain rates causes the transition temperature to exceed  $350^\circ\text{C}$ , as indicated by the data of Fig. 1 (1). The onset of embrittlement, however, is near  $150^\circ\text{C}$ , independent of strain rate. Similarly, the onset of embrittlement in aluminum tested in mercury remains constant, at the melting point of mercury, while the transition temperature increased by some  $70^\circ\text{C}$  as strain rate increased from  $4 \times 10^{-5} \text{ sec}^{-1}$  to  $0.503 \text{ sec}^{-1}$ , see Fig. 4 (15). Aluminum displayed an extremely sharp transition temperature region ( $\sim 7^\circ\text{C}$ ) and the fracture mode was intergranular, independent of strain rate. Other systems exhibiting an (linear) increase in recovery temperature with

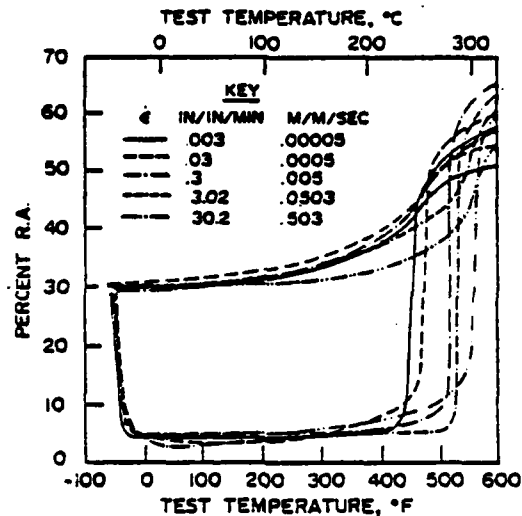


Fig. 4. Embrittlement of 2024-T4 aluminum by mercury at several strain rates (15).

increasing strain rate include Zn-Hg (1), Zn-Ga (1), Ti55A/Cd (16), 2024Al/Hg-3%Zn (17), and 4145 steel/Pb (15).

The pattern of behavior of the recovery from MIE suggests that the substrate properties control ductility, rather than a desorption reaction (17) or a transport problem (18). This approach is supported by work on zinc coated with cadmium (1). At temperatures above the cadmium melting point, the yield stress of zinc at ordinary strain rates lies below the fracture strength in cadmium. Upon increasing the strain rate by a factor of ten, the yield stress was increased and embrittlement was observed.

#### Specificity

The strain-rate data illustrate two important points: that apparently nonsusceptible metals at any temperature may in fact be severely embrittled by a liquid (or solid) metal environment if the strain rate is increased sufficiently, and that the melting point of the embrittler at best can only suggest the temperature of maximum susceptibility. In the case of Armco iron tested in tin, cadmium, bismuth or Pb-Bi, the maximum embrittlement occurred near 350°C, even though the embrittler melting points differ by several hundred degrees (20). These findings cast serious doubt upon the significance of "specificity", since so many embrittlement and non-embrittlement couples reported and summarized in the literature have been identified on the basis of experiments at one or a few temperatures, usually at a single constant strain rate. Similar caution must be exercised in the choice of substrate grain size, and perhaps the



nature of the environment surrounding the liquid metal (20).

7

### Transport Mechanisms

There has been some controversy in the literature concerning the mechanism of embrittler transport to a crack tip. When present as a liquid, the embrittler is generally believed to approach the crack tip by bulk liquid flow; however, access to the crack tip itself has been thought to occur by some rapid diffusional process, such as second monolayer surface diffusion (21). Gordon (22) has recently proposed, however, that liquid zinc can penetrate to very near the tip of a sharp crack in 4140 steel, based upon both direct observation and calculations. Gordon further calculated that liquid flow transport is very rapid for all liquid metal embrittlers, even in cracks of very small tip radii. However, for high vapor pressure liquids such as zinc, cadmium and mercury, vapor transport also may contribute to embrittlement.

Below the embrittler melting point, transport by bulk liquid flow is, of course, impossible, but transport through the vapor phase also seems to be unlikely for most embrittlers (other than zinc, cadmium and mercury). This is largely a consequence of very low vapor pressures at their respective melting points for lead, bismuth, lithium, indium, tin and gallium (2). Solid state diffusion is left as the only viable transport mechanism. Grain boundary diffusion and first monolayer diffusion of the embrittler over the substrate are likely to be too slow. Second monolayer or multiple monolayer self-diffusion would then be necessary to avoid embrittler-substrate diffusion interaction. Surface self-diffusion rates of  $10^{-3}$  to  $10^{-6}$  cm<sup>2</sup>/sec have been measured (23), in good agreement with apparent diffusivities inferred from crack propagation rates in steel.

### EMPIRICAL PREDICTIONS OF SUSCEPTIBILITY

Several approaches have been used with varying success in recent years to predict or rationalize susceptibility of specific metals to embrittling environments. Kelley and Stoloff (24) proposed that cohesion of the solid is lowered or shear is enhanced in the presence of a liquid metal to a degree determined by the amount of the solid-liquid bond energy. The Engel (25) - Brewer (26) thermodynamic cycle was used to estimate the interaction energy (IE) between the atoms of the two metals forming an embrittlement couple. [A similar approach, developed independently, has been applied to hydrogen embrittlement of austenitic stainless steels (27).] IE represents the energy released by one-to-one bond formation between atoms of the liquid and the solid, neglecting any effects relating to less than full surface coverage. The fracture surface energy (FSE) was assumed to be proportional to the bond energy, so that the ratio of the solid-liquid bond energy to the solid-solid bond energy (assumed equal to the atomization energy) is a measure of the reduction of

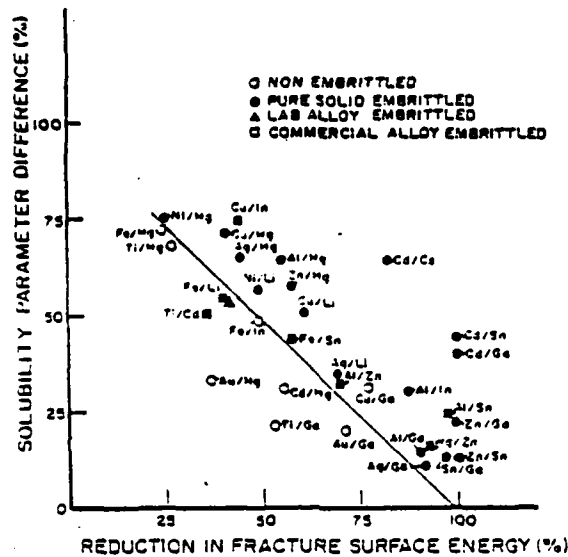


Fig. 5. Calculated reduction in fracture surface energy relative to solubility parameter for various substrate/environment combinations (24).

FSE in the presence of the liquid. The likelihood of embrittlement was related directly to a second factor, the solubility parameter, defined as the square root of the sublimation energy per unit volume; a small difference in solubility parameters (28) defined as  $\delta = (\Delta E_1/V_1)^{1/2}$  where  $\Delta E_1$  = heat of sublimation and  $V_1$  = molar volume of solid and liquid is indicative of a large mutual solubility. It was proposed that a plot of solubility parameter difference vs. %reduction in FSE could identify the boundary between embrittlement and no embrittlement, Fig. 5 (24). Embrittlement is favored by increased reduction in FSE and by reduced mutual solubility. Reduced FSE was considered to arise from decohesion, Fig. 6.

This model was recently tested by Roth et al (9) who calculated reduction in FSE and solubility parameter differences for three couples: Al-Bi, Al-Cd and Al-Pb; embrittlement data for Al-Bi and Al-Pb appear in Fig. 2. The reductions in fracture surface energy for these systems were calculated to be 82, 67 and 80%, respectively. Relative solubility parameter differences between aluminum and bismuth, cadmium and lead were computed to be 44, 48 and 40%, respectively, consistent with small solubilities of these elements in aluminum. The data for these alloys all fell within the embrittling range of Fig. 5, so that embrittlement was successfully predicted. However, the calculations did not predict the correct order of the relative severity of embrittlement of aluminum with the three environments. The predicted loss in cohesion caused by lead and bismuth is nearly identical, and larger than that predicted for cadmium (and that for mercury, which is known to cause much more severe

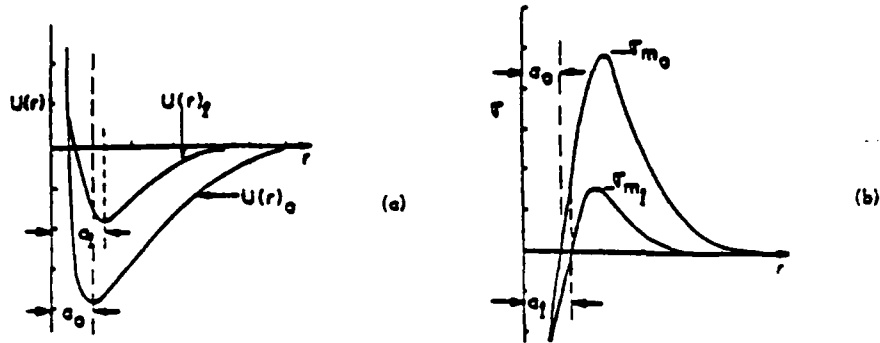


Fig. 6. Schematic diagram of decohesion model, showing proposed influence of liquid metals on bond strength,  $\sigma_m$ , and energy to rupture bonds at crack tip,  $U(r)$ . (10)

embrittlement in aluminum); however, bismuth was much more potent an embrittler than lead. Thus the model was concluded to be inadequate in predicting susceptibility to embrittlement. It should be emphasized, however, that the demarcation between embrittlement and non-embrittlement conditions shown in Fig. 5 is sensitive to metallurgical variations such as grain size and environmental considerations such as temperature and strain rate, consistent with the requirements of Eq. (2) (5,24). It was concluded in an earlier paper that "specificity is a matter of degree: strong interactions will lead to embrittlement under a variety of test conditions, while weak interactions require a very precise combination of conditions" (3). This caveat must be applied to any model of embrittlement that relies solely upon bulk thermodynamic or physical properties.

Several alternative approaches to predicting susceptibility of LME consider solely the reduction in surface energy,  $\gamma$ , due to the presence of a liquid at the crack tip. According to Griffith (29), for a body stressed elastically, and fracturing with no dissipative processes other than forming a new surface of energy per unit area,  $\gamma_s$ ,

$$\sigma_F = \sqrt{\frac{2E\gamma_s}{\pi a}} \quad (\text{plane stress}) \quad (3)$$

where  $E$  is Young's modulus and  $a$  is half-crack length. Later, Cottrell (12) and Petch (13) independently showed that crack nucleation at the yield stress could be described in terms of dislocation pile-ups coalescing to form a crack nucleus by Eqs. (1) and (2), except that the appropriate  $\gamma$  to use in Eq. (2) is the effective surface energy,  $\gamma_{eff}$ , which includes the effects of plastic work.

When attempts are made to explain embrittlement phenomena through a reduction in surface energy, objections arise, based upon

the seeming difficulty in explaining how the plastic work accompanying fracture, which far exceeds the true elastic surface energy in metals, can be decreased by the environment. Orowan (30) had suggested that plastic work and elastic surface energy terms are additive quantities. This apparent problem, in fact, was solved twenty years ago, although apparently not recognized as recently as 1977 by Birnbaum (31) and in 1980 by Jokl et al (32).

It was pointed out initially by Gilman (33), and later by Stoloff and Johnston (10) and Westwood and Kamdar (21) in the context of liquid metal embrittlement, that when a plastic zone is present at the crack tip, the radius,  $\rho$ , of the zone will influence the effective energy to fracture the material,  $\gamma_{eff}$ . The two surface energies are proportional:

$$\gamma_{eff} = \frac{\rho \gamma_s}{a_0} \quad (4)$$

where  $a_0$  is the substrate lattice parameter. On this model, the metal embrittler atoms lower  $\gamma$ , as shown in Fig. 6, and by causing the crack tip to remain sharp during propagation,  $\gamma_{eff}$  is reduced proportionally. This approach is much more straightforward and tractable than the more involved path taken by Jokl et al (32) to come to the same conclusion.

The application of thermodynamic surface energy measurements to embrittlement will now be considered. When a perfectly brittle single crystal is fractured in an inert atmosphere,  $\gamma_{eff}$  is approximated by the solid-vapor surface energy  $\gamma_{SV}^0$ . For intergranular fracture of a polycrystalline alloy

$$2\gamma = (2\gamma_{SV}^0 - \gamma_{GB}^0) \quad (5)$$

where  $\gamma_{GB}^0$  is the energy of the grain boundary. When liquid metal is present, the equations are  $\gamma = \gamma_{SL}$  for single crystals (or trans-crystalline failure in polycrystals) and  $\gamma = 0.5(2\gamma_{SL} - \gamma_{GB})$  for grain boundary fractures. For wetting systems  $\gamma_{SL} < \gamma_{SV}$  and a coefficient of embrittlement,  $\eta_1$

$$\eta_1 = \frac{\gamma_{SL}}{\gamma_{SV}} \quad \text{or} \quad \frac{2\gamma_{SL} - \gamma_{GB}}{2\gamma_{SV} - \gamma_{GB}} \quad (6)$$

may be defined (35,36). The effective surface energy,  $\gamma_{eff}$ , is simply proportional to the appropriate value of  $\gamma$  defined above. As  $\eta_1$  decreases, the stresses necessary to initiate or propagate cracks decrease, and the ductile to brittle transition temperature increases.

Roth et al (9) have applied this macroscopic model to the grain boundary fracture of aluminum induced by liquid inclusions. The

severity of embrittlement was related to the energies defined above in terms of the fractional reduction in work of fracture,  $\Delta W/W$ , due to the presence of the liquid:

$$\frac{\Delta W}{W} = \frac{2\gamma_{SV}^{\circ} - \gamma_{GB}^{\circ} - (2\gamma_{SL} - \gamma_{GB})}{2\gamma_{SV}^{\circ} - \gamma_{GB}^{\circ}} \quad (7)$$

The grain boundary energy of most pure metals and alloys is approximately one-third of  $\gamma_{SV}$ , and  $\gamma_{GB}$  can be expressed in terms of the dihedral angle,  $\theta$ , reducing  $\Delta W/W$  to the following:

$$\frac{\Delta W}{W} = 1 - 0.2(\sec \theta - 1) \left( \frac{\gamma_{GB}}{\gamma_{GB}^{\circ}} \right) \quad (8)$$

Roth et al (9) concluded from the large dihedral angles observed with lead, cadmium, and bismuth on aluminum that these elements do not strongly adsorb at grain boundaries, so that  $\gamma_{GB}/\gamma_{GB}^{\circ}$  is about 1. Then  $\Delta W/W$  is a function of  $\theta$  only, resulting in  $\Delta W/W = 0.88$  for Al-Bi, 0.86 for Al-Cd and 0.81 for Al-Pb. These values of  $\Delta W/W$  are in the same order as the severity of embrittlement noted in these materials, as measured by the impact energy absorbed when the inclusions are liquid (1.5J for Al-Bi, 1.8J for Al-Cd and 5.4J for Al-Pb); on this basis, the surface energy approach was considered applicable to LME. In extreme cases, the dihedral angle,  $\theta$ , approaches zero and the liquid metal will penetrate grain boundaries even if the solid is unstressed. In this case  $2\gamma_{SL} \leq \gamma_{GB}$ . Al-Ga is a system of this type.

Nicholas and Old (36) also have recently advocated use of  $\gamma$ , determined from wetting studies, to correlate with fracture data. For example, ratios of  $\gamma_{SL}/\gamma_{SV}$  measured in moderate vacua are in reasonable agreement with reductions in the effective fracture energy. These observations suggested that ratios of  $\gamma_{SL}/\gamma_{SV}$  of less than 0.5 are associated with LME of zinc (e.g.  $\gamma_{SL}/\gamma_{SV} = 0.41$  for embrittling mercury and 0.27 for embrittling gallium, but  $\gamma_{SL}/\gamma_{SV} = 1.16$  for non-embrittling sodium and 0.61 for non-embrittling bismuth). However,  $\gamma_{SL}/\gamma_{SV}$  is 0.5 for non-embrittling cadmium, which is very close to the ratio of 0.48 noted for embrittling lead. It is doubtful that any model could so sharply define an embrittlement condition, especially in view of the role of metallurgical variables. Also, no explanation of the significance of a ratio of 0.5 was offered, suggesting that the dividing line is totally arbitrary.

Another problem with the surface energy model is that it does not predict changes in bond strengths with crystallographic orientation. Studies on several metals suggest that surface energies differ by only a few % with orientation, while a difference in bond strength of some 30% between [001] and [111] was inferred for fracture of

Several authors (1,19,37,38,39) have suggested that the surface energies of pure elements may be connected with high heats of vaporization or high heats of mixing,  $\Delta H_m$ . Couples which display a high positive  $\Delta H_m$  would not be expected to form bonds; the interfacial energy is then expected to be high and embrittlement is not observed. Negative values of  $\Delta H_m$  imply preferred bonding between environment and substrate, and either significant material solubility or compound formation will occur. Only when  $\Delta H_m$  is small and positive is embrittlement to be expected. Limited success in rationalizing embrittlement of zinc by six low melting metals has been claimed, see Table 1 (1). However, the correct order of embrittling tendency was not predicted. Moreover, the heat of mixing approach predicts non-embrittlement of aluminum by lead and bismuth (19), contrary to recent experimental results (9). Worse yet, Tetelman and Kunz (19) identified hydrogen "conclusively" as a non-embrittler of aluminum, contrary to many recent published results (40). A significant problem in evaluating the model for other alloy systems is the relative sparseness of  $\Delta H_m$  data. Nevertheless, the results obtained to date with this model do not appear to be promising; in fact, Gilman (41) has pointed out that heat of mixing data provide no better than 50% success in predicting embrittlement; i.e. there is no predictive capability. Perhaps the situation could be improved by combining the heat of mixing data with solubility parameter differences to establish a boundary between embrittling and non-embrittling conditions.

Toropovskaya (42) has related the heat of fusion,  $H_f$ , to interatomic bonding, suggesting that:

Table 1. Susceptibility and  $\Delta H_m$

<u>Couples</u>	<u><math>\Delta H_m</math></u>	<u>Embrittlement</u>
Zn-Bi	19	Yes
Cd	4	Yes
Ga	0	Yes
Hg	4	Yes
In	12	Yes
Sn	4	Yes
Cu-Na	37	No
Cu-Li	-39	Yes-Compds
mild steel - Li	95*	Yes-decarb, $\Delta H_m$ typical
mild steel - Na	236*	No
Al-Cd	13	Yes
Al-Zn	2	Yes

\* embrittlers of iron tend to have fairly high  $+\Delta H_m$ .

$$\frac{H_{FL-S}}{H_{FS}} = \frac{\sigma_{FL-S}}{\sigma_{FS}} = \eta_2 \quad (9)$$

where  $H_{FL-S}$  is the heat of fusion of a liquid-solid solution. Good agreement for several embrittling elements on copper was claimed between the ratios of the thermodynamic and fracture stress quantities. No data for other than copper substrates have been reported.

Proponents of each of the empirical systems outlined above can claim limited success, sometimes with one substrate, others with a number of base metals. However, there is still no completely satisfactory system for predicting embrittlement couples. Moreover, none offer any insight into the nature of the precise environment-substrate interaction that leads to embrittlement.

#### MECHANISMS OF CLASSICAL METAL-INDUCED EMBRITTLEMENT

The precise interaction between atoms of an embrittler and a stressed substrate that leads to embrittlement remains unknown. The calculational schemes outlined previously, through which likelihood and degree of embrittlement may be predicted with varying degrees of success do not shed much light on this matter, nor do the transport mechanisms also outlined earlier. We shall now briefly review several proposed mechanisms of embrittlement that focus upon events at the crack tip, as follows:

- 1) decohesion
- 2) enhanced shear
- 3) stress-assisted dissolution
- 4) embrittlement of grain boundaries by diffusion

#### Decohesion

The most widely accepted theory of both metal-induced and hydrogen-induced embrittlement postulates that chemisorbed embrittler atoms lower bond strength at the crack tip, thereby facilitating both nucleation and propagation of a crack (10,21). The proposed reduction in cohesion due to an embrittler atom is shown schematically in Fig. 6 (10). For a perfectly elastic fracture the lowering of bond strength has two equivalent effects: the stress to rupture the bonds is decreased and the energy obtained by integrating under the force-distance curve (i.e. the bond energy or true elastic surface energy,  $\gamma$ ) is reduced. Note that the diagram implies also reduced elastic modulus at the crack tip. Oriani (43) has pointed out that in non-ideally elastic situations (i.e. most structural metals in contact with liquid metals or hydrogen), a reduction in cohesive stress need not be equivalent to reducing surface (cohesive) energy. For this reason, he has suggested that attention be directed towards the bond strength as being the critical parameter.

The decohesion model, in spite of its wide acceptance, is open to a number of criticisms, stemming from the inability of researchers to define the interaction that ultimately leads to enhanced bond breaking.

If there is indeed a finite number of specific embrittler-substrate combinations, the decohesion model cannot predict such specificity. However, as pointed out by others (1,44) and demonstrated earlier in this review, the presence or absence of embrittlement depends sensitively upon the choice of test variables such as temperature and strain rate, and metallurgical variables such as grain size and stacking fault energy. This factor impacts equally on other proposed embrittlement mechanisms, to be outlined below, and therefore cannot be the definitive factor in rejecting any embrittlement model.

A more specific criticism of decohesion may be found in the relatively wide occurrence of delayed failure among embrittlement couples, as recently compiled by Gordon.(45) In the majority of cases, e.g. 4340 steel in cadmium (46) and Cu-2%Be in mercury (47), readily recognizable delayed failure (type A behavior) was observed, but in several instances, all involving mercury or mercury-indium environments on zinc (48), cadmium (48), silver (49), or aluminum (49), delayed failure did not occur (type B behavior). In type B situations, there appears to be a critical stress above which failure is virtually "instantaneous" (less than 1-2 sec) but below which no failure is observed. However, Gordon suggests that even in the latter category very rapid delayed failure may be occurring, i.e. that crack nucleation occupies most of the very short failure time. An incubation period, during which no crack greater than about 0.01 mm long could be detected, was observed in delayed failure experiments on unnotched 4140 steel, in the quenched and tempered condition, embrittled by either liquid or solid indium. Other evidence on this point is conflicting: an incubation period having been reported in some, but not all, systems studied. It is difficult to reconcile delayed failure, especially with an incubation time, with a surface-induced decohesion phenomenon which should occur instantaneously upon contact of the embrittler atoms with a crack nucleus.

An added criticism of the decohesion model as applied to hydrogen effects on fracture has been made by Clark et al (50) who showed that the surface free energy of a Ni-300 ppm hydrogen solid solution is nearly equal to that of pure nickel. However, a decrease in grain boundary energy of about 20% due to hydrogen in solution was measured. It was concluded that hydrogen can decrease the work for intergranular or transgranular fracture due solely to adsorption effects and not by significantly altering the lattice potential between the solvent atoms. The implications of these findings for metal-induced embrittlement are not yet clear. Similar measurements of lattice energies of metal in the presence of liquid metals do not



seem to have been made. Yet the doubt cast upon decohesion of nickel by hydrogen, a known embrittler, does not seem to bode well for the decohesion model of LME.

### Enhanced Shear

The most sustained criticism of the decohesion model as applied to both LME and hydrogen embrittlement is based upon metallographic and fractographic observations of embrittled samples, most notably by Lynch (51-55). Decohesion implies a cleavage mechanism of fracture in which atomic bonds defining a crack tip are ruptured by forces acting normal to the crack plane, leading either to crystallographic cracking or to grain boundary separation. Careful fractographic examination of many LME couples has, however, revealed dimples in the fracture surfaces and there is metallographic evidence of considerable plastic strains accompanying fracture, as will be described in the following section. For example, fracture surfaces in polycrystalline cadmium embrittled by gallium reveal what appear to be cleavage facets at low magnification, Fig. 7 (a), but at higher magnification numerous small dimples may be observed, as shown in Fig. 7 (b) (52). Fractographic examination of embrittled aluminum single crystals tested under cyclic loading further showed that cracks propagated along cube planes in the close-packed  $\langle 110 \rangle$  directions, see Fig. 8 (55); and that extensive slip seemed to occur on  $\{111\}$  planes intersecting the crack tip. On the basis of these observations, Lynch suggested that chemisorption facilitated nucleation of dislocations from crack tips, Fig. 9 (51,53,55).

Several means by which weak chemisorption can facilitate dislocation nucleation have been suggested. The transfer of electrons

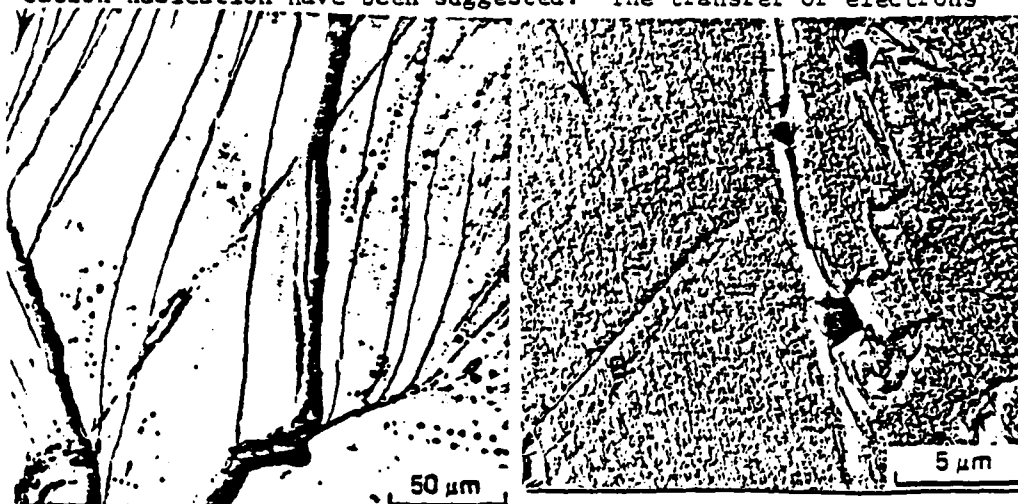


Fig. 7. Fractograph of cadmium after fracture in liquid gallium. (a) apparent cleavage facets; (b) shallow elongated dimples (after Lynch).

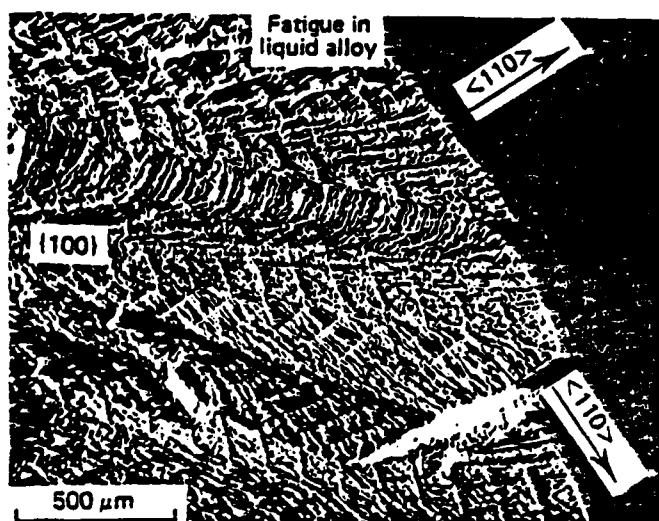


Fig. 8. Scanning electron micrograph of solution treated aluminum alloy, showing  $\{100\}$  facets produced by fatigue. Zigzag crack fronts due to growth in different  $\langle 110 \rangle$  (55).

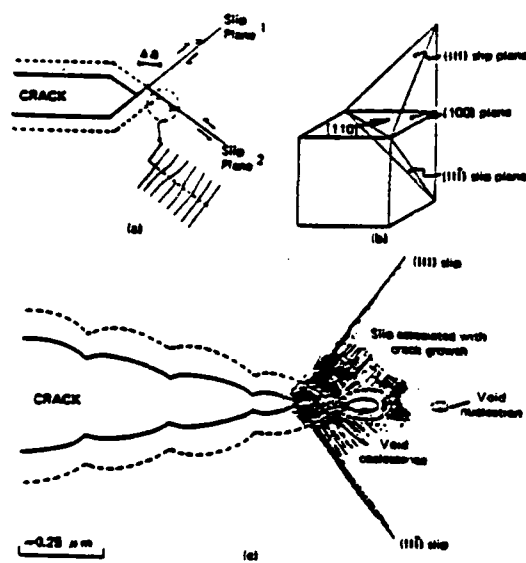


Fig. 9. Schematic diagram showing:  
 (a) crack growth,  $\Delta a$ , by alternating shear on two slip planes; (b) orientations of planes and direction in fcc, showing that alternate slip on  $\{111\}$  produces crack growth along  $\langle 110 \rangle$ ; (c) general slip, in addition to alternate slip, producing nucleation and growth of voids ahead of crack. Dotted line shows crack position after growth  $\Delta a$  (53).

from adsorbed species to atoms of the substrate at the surface may locally increase the electron density and thereby increase the repulsive force between adjacent surface atoms. Reduced cohesion between surface atoms should thereby enable shear between surface atoms to occur more readily. Stoloff and Johnston (10) proposed that the localized Young's modulus (and therefore the shear modulus) at a crack tip may be reduced by an adsorbing species, see Fig. 6. Krishtal made the same point in 1970 (56), as did Matsui et al in 1977 (57) and 1979 (58), the latter in reference to appreciable softening of high purity iron in the presence of hydrogen. Birnbaum has, in fact, reported a substantial drop in the shear modulus of nickel, as measured in a torsion pendulum (31). Oriani and Josephic (59), faced with this evidence, conclude that softening by hydrogen can sometimes arise from a reduction in interatomic bond strength at the dislocation cores, leading to a lowering of the Peierls barrier to dislocation motion. Nevertheless, these authors continue to adopt the view that decohesion is responsible for embrittlement, citing other examples of softening attributable to an increase in density of microvoids or internal pressurization effects. Thus, although it is now widely agreed that dislocation nucleation or motion can be facilitated by hydrogen and perhaps by liquid metals, there is still disagreement about the significance of such observations.

A critically important feature of suggestions as to the role of the environment is the concept that moduli are reduced only in the immediate vicinity of the environment. There is no measurable effect of liquid metals on bulk elastic or plastic properties, except that the fracture stress and/or strain are reduced. It seems more likely, based upon the widely divergent fracture observations outlined above, that both tensile and shear strength of interatomic bonds are decreased by films causing LME or SMIE. The observed fracture morphology will then depend upon such additional factors as the availability of a low energy cleavage plane, segregation of impurities to grain or subgrain boundaries, and the orientation of the maximum principal stress axis relative to individual crystals. Similarly, Clum (60) has suggested that enhanced dislocation nucleation in iron at surfaces in the presence of adsorbed hydrogen can lead to barrier formation by interaction of these dislocations with slip dislocations, leading to embrittlement. The distinguishing criteria were suggested to be the number of dislocations and their Burgers vector in any region of the solid. The results of Wanhill (61) on fracturing of a high strength titanium alloy in mercury also are consistent with a model based on liquid metal facilitating slip on the  $\{10\bar{1}0\}$  which intersect (0001) cleavage surfaces.

Additional evidence that enhanced shear may contribute to metal-induced embrittlement may be found in the work of Goggin and Moberly (62) on the tensile behavior of single crystal aluminum foils exposed to gallium. Foils generally failed in a ductile manner, except for short (few micron) segments which rapidly propagated before

blunting occurred. Subsequent failure was by ductile shear. Cracks did not initiate at dislocation pileups, at grain boundaries (in polycrystals) or at slip band intersections. In the case of cyclic loading of mercury-coated copper, Tiner (63) has reported that the crack apparently propagates at high velocity by transcrystalline shear. This observation also is in accord with an environment-assisted shear model of LME.

In an effort to approach the mechanism of embrittlement from an entirely different point of view, efforts have been made to embrittle amorphous metallic alloys either with liquid metals or with hydrogen introduced cathodically (64). Since amorphous alloys deform and fracture in inert environments by a shear process, it was anticipated that embrittlement by any of the selected environments could lead to improved understanding of the relevance of shear processes to environmentally-induced fracture.

Table 2 lists the compositions of several amorphous alloys tested in mercury or Hg-In environments. When tested in air in tension at room temperature, all of the alloys are macroscopically brittle; but as temperature is increased appreciable plastic deformation occurs. Plastic deformation occurs by intense shear on planes or surfaces inclined at about 45° to the stress axis, see Fig. 10 (a). Deformation is quasi-viscous in nature, and therefore no work hardening occurs. Initiation of shear in one of the bands leads to fracture at the yield stress, with microscopic strains of the order of 1000% or more. Fracture surfaces in air reveal a veining pattern, see Fig. 11 (a). When these alloys are tested in the presence of a liquid metal, fracture stresses are reduced, Table 2, the shear pattern on the specimen surfaces changes, Fig. 10 (b); the fractographic features, at least at low magnification, appear to be very brittle, Fig. 11 (b). However, at high magnification the veining pattern reappears, Fig. 11 (c), showing that only the scale of the pattern has changed. Similar effects are noted in the same amorphous metals after cathodic charging. Consequently, it appears that not only is enhanced shear a viable mechanism for LME of amorphous metals, but that it may account for hydrogen embrittlement of these alloys as well.

Table 2. Embrittlement of Amorphous Alloys at 25°C (64).

Alloy	$\sigma_F$ (GPa)		
		Hg	Hg-In
$Fe_{81.5}B_{14.5}Si_4$	$1.90 \pm 0.26$	$1.36 \pm 0.5$	$1.26 \pm 0.33$
$Fe_{81.5}B_{13.5}Si_{2.5}C_{2.5}$	$1.50 \pm 0.37$		$1.03 \pm 0.48$
$Fe_{49}Ni_{40}P_{14}B_6$ (2826)	$1.30 \pm 0.21$		$1.18 \pm 0.16$
$Fe_{40}Ni_{38}B_{18}Mo_4$ (2826 MB)	$1.60 \pm 0.19$		$1.48 \pm 0.17$

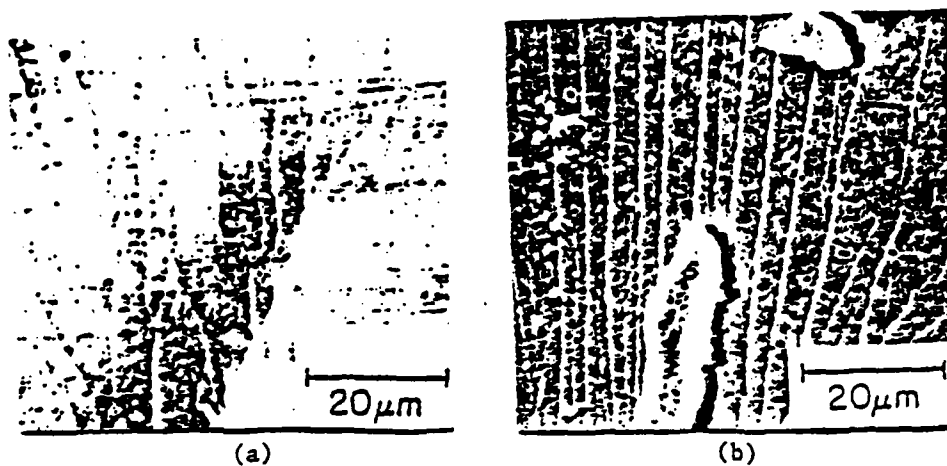


Fig. 10. Shear bands near crack tips in bend specimens of amorphous FeBCSi, tested at 25°C (64).  
(a) air; (b) Hg-In.

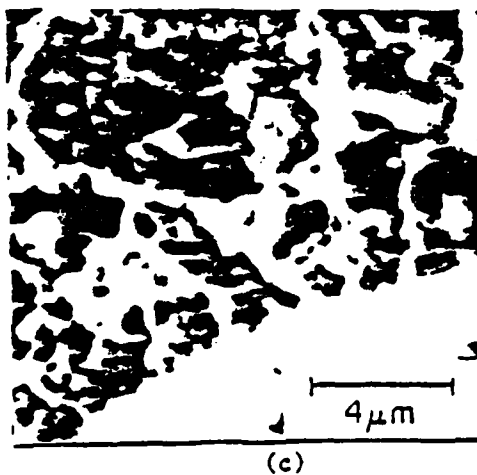
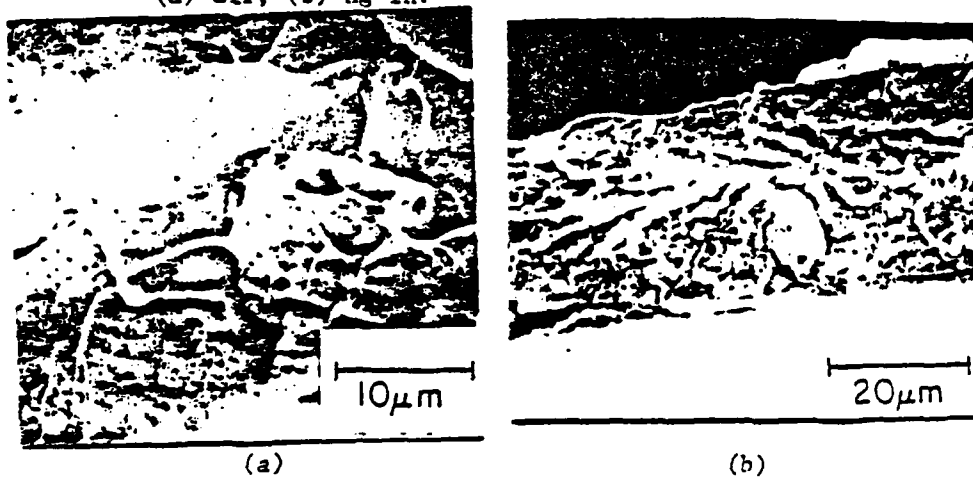


Fig. 11. Fractographs of amorphous FeCBSi tested in tension at 25°C (64).  
(a) air; (b) Hg-In (low magnification); (c) Hg-In (high magnification).

A further critical test of the enhanced shear mechanism involved bending of one of the amorphous alloys (Metglas 2826) with liquid lithium on the compressive or tensile side of the bend sample. Severe embrittlement was noted in either case, providing clear evidence that a state of tensile stress is not necessary for embrittlement to occur. This observation is perfectly consistent with a fracture process depending upon shear only, but cannot be explained by a decohesion model. However, this result does not explain the apparent lack of reports of embrittlement of crystalline metals in bending or compression, except for a few cases in which secondary tensile stresses developed as a result of bending. Certainly more attention should be directed to state of stress in embrittlement testing to clarify this point.

In spite of the apparent success of the enhanced shear model with regard to amorphous metals, there remain serious criticisms of the applicability of the model to crystalline metals:

- a) The formation of microvoids ahead of a crack tip should not be influenced by liquid metal atoms at or just behind the crack tip.
- b) No reasonable mechanism for delayed crack initiation is offered, since the alteration of surface structure of bonding should be virtually instantaneous if it is caused by embrittler atom adsorption, particularly if the embrittler is in liquid form (45).
- c) Slip on alternating planes is highly unlikely in zinc and cadmium, which deform solely on the basal plane for most crystal orientations.
- d) Fracture of gallium-embrittled aluminum single crystals always occurred on {100} for four widely differing initial orientations (37). It is not at all apparent how alternating shear on two {111} slip planes could occur in the amounts necessary to produce the same fracture plane in each case (31).

The questions surrounding both the decohesion and enhanced shear models are sufficient to require much more experimental and theoretical work before either mechanism can be accepted for crystalline metals.

#### Dissolution

Robertson (16), and later Glikman et al (65,66), proposed that rapid localized dissolution of highly stressed atoms at the leading edge of a crack is the cause of crack propagation in LME. The dissolved material would need to be carried away by diffusion through the liquid. The problems with this approach have been well known for some time:

- (a) dissolution would have to be rapid enough to account for

crack propagation rates measured in cms/sec; this is highly unlikely.

- (b) increasing temperature should lead to increased embrittlement; in fact, the reverse is observed with most embrittlement couples, see Figs. 1, 2, 4.
- (c) crack initiation and propagation are not separable events, yet the embrittlement of 4140 steel by indium suggests that there are distinctly different initiation and propagation stages of both SMIE and LME (45).
- (d) the mechanism can hardly account for SMIE at all, but in any case would predict an abrupt change in temperature dependence of crack initiation at the embrittler melting point; this also is contrary to results of indium embrittlement of 4140 (45).
- (e) the severity of embrittlement should increase with increasing solubility of the substrate in the liquid; this, of course, violates one of the principal empirical prerequisites for LME, namely limited mutual solubility is required for embrittlement to occur.

#### Grain Boundary Embrittlement

Krishtal (56) has proposed that LME is composed of a two step process: embrittler atoms must initially diffuse along grain boundaries in the substrate to a critical depth and concentrate on the boundaries, which are then embrittled. Dislocations produced by strains resulting from the embrittler atoms' presence as well as dislocations produced by lowering of the base metal surface energy are responsible for the embrittlement. Ignoring the rather fuzzy references to dislocation generation, Gordon (45) has adopted and extended the Krishtal mechanism to explain SMIE. Embrittler atoms first change from the adsorbed to the dissolved (in the surface) state, and subsequent penetration occurs along grain boundaries or other preferred paths. Both steps are accelerated by the applied stress. Crack nucleation eventually occurs in the embrittled zone when the proper concentration of embrittler atom has been reached. Once the crack forms, it grows rapidly until a visible crack is produced, or until the length of the crack is such that the transport process becomes rate controlling.

The principal advantage of such a mechanism is the natural prediction of delayed failure phenomena: the model also provides reasonable estimates for the apparent activation energy for crack initiation with indium on 4140 steel. The model does not address specificity, but can explain the onset of embrittlement and the restoration of ductility at some higher temperature on the following basis: as temperature increases the rates of solution and grain boundary diffusion first become sufficiently high to cause crack initiation near the embrittler melting point,  $T_m$ . At temperatures higher than  $T_m$ , volume diffusion from the boundaries into adjacent grains reduces

the grain boundary concentration, eventually producing the characteristic brittle-ductile transition.

Gordon (45) also suggests that the grain boundary embrittlement model can account for strain rate, solute, grain size and cold work effects, all due to the influence of these variables on volume diffusion, e.g. at higher strain rates, higher temperatures are needed to dissipate grain boundary penetration zones. Decreasing grain size reduces pileup-induced stress concentrations at grain boundaries, requiring greater embrittler penetration to accomplish embrittlement, while increasing cold work increases dislocation density in base-metal grains, providing more short-circuit volume diffusion paths to dissipate embrittler concentrations at grain boundaries.

This mechanism, unfortunately, provides no insight into the many recorded instances of transgranular (or single crystal) embrittlement noted in the literature, nor can it explain the embrittlement of amorphous alloys. Furthermore, and perhaps most importantly, pre-exposure to the environment, followed by testing in an inert medium, should cause embrittlement; in fact, this is rarely the case, except for the well known Al-Ga system in which diffusion along grain boundaries is very rapid (67) and for single crystals of zinc in contact with mercury or gallium which display embrittlement due to the formation of a brittle alloy layer (68).

#### SIMILARITIES AMONG EMBRITTLEMENT PHENOMENA

In recent years there has been renewed interest in possible links between embrittlement phenomena: e.g. impurities that promote temper embrittlement also have been shown to increase the susceptibility of steels to hydrogen embrittlement. More importantly, there have been several cases where hydrogen embrittlement and MIE have been closely linked (19,51,54,69,70), both in crystalline and amorphous substrates, as pointed out earlier. This linkage has been based on the following conditions which appear to be necessary for embrittlement of crystalline metals with both species:

- a) tensile stress must exist in the base metal (this has now been cast in doubt for amorphous metals)
- b) pre-existing cracks or stable obstacles to dislocation motion must be present
- c) embrittling species must be present at the obstacle and subsequently at the tip of the propagating crack
- d) low mutual solubilities, little tendency to form compounds and strong binding energies are characteristic of embrittlement couples.

In the case of steels, certain other similarities also have been noted (54,71):



- 1) embrittlement tends to increase with increasing strength level.
- 2) elements that form stable compounds with the solid, when added to the liquid, inhibit MIE, just as oxygen inhibits embrittlement by hydrogen.
- 3) the temperature sensitivities of HE and MIE are similar, with maximum embrittlement noted at some intermediate temperature (room temperature for HE, generally near the melting point of the liquid for MIE, see Figs. 1, 4.
- 4) factors that favor planar glide increase susceptibility.
- 5) similar crack growth rates have been observed for D6AC steel in mercury and in dissociated hydrogen (54).

Temper embrittlement (TE), HE and MIE also may be linked in the common effects of certain impurities, most notably antimony and tin, in promoting fracture. Breyer and Johnson (72) have noted the apparent connection between TE and MIE, while Yoshino and McMahon (73) have noted a relation between conditions favoring TE and HE, thereby suggesting that there may be a common predisposition of certain steels to all three types of embrittlement. It should be pointed out, however, that even if such a common predisposition exists, there need not be a single mechanism by which bond strength (or fracture energy) is reduced.

#### EFFECTS OF ALKALI METALS ON MECHANICAL PROPERTIES

Sodium and lithium are to be used in contact with structural materials in the liquid metal fast breeder reactor and in controlled fusion devices, respectively. Much of the research on suitable containment materials for high temperature lithium has focussed on ferrous alloys, including carbon, low alloy and stainless steels. In addition, there are some limited data on embrittlement of nickel and palladium-based alloys.

Two characteristics of lithium-induced embrittlement differ from those associated with most embrittling metals. Firstly, the degree of embrittlement produced by lithium is very sensitive to the atmosphere in which the lithium is applied, see Fig. 12 (74), due probably to differences in moisture content as well as due to the variation in wetting behavior of the lithium. Secondly, lithium can cause embrittlement at stresses much below the apparent or macroscopic yield stress of the substrate. In fact, the ratio of wetted fracture stress to unwetted yield stress for Ni-Cu and Pd-Ag silver alloys can be as low as 0.2 (74). This contrasts with the situation for most crystalline substrates, for which the wetted fracture stress is equal to or greater than the unwetted yield stress. Embrittlement noted with lithium often is concentrated at grain boundaries (75), leading to the conclusion that decarburization at grain boundaries can facilitate crack growth. However, recent work on amorphous alloys has demonstrated severe lithium embrittlement of  $\text{Fe}_{49}\text{Ni}_{40}\text{P}_{14}\text{B}_6$  in the

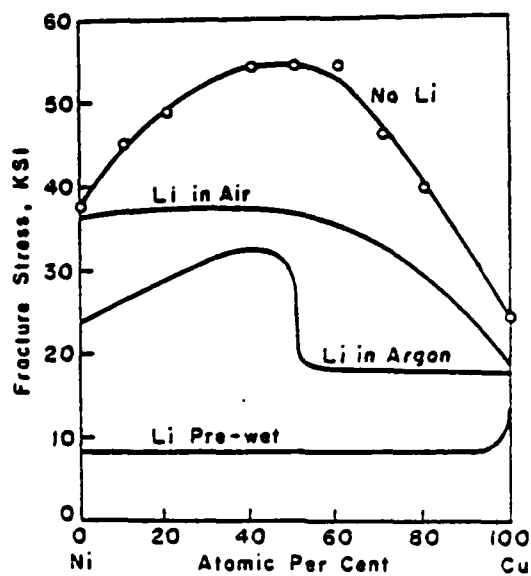


Fig. 12. Influence of test conditions on fracture stress of Ni-Cu alloys in molten lithium (74).

absence of both grain boundaries and carbon (76). Therefore lithium must have an intrinsic effect on bond strength as well.

A limited amount of fatigue data on steels in alkali metal environments is available. A 2-1/4Cr-1Mo steel tested in lithium containing 1.5%N shows a much higher crack growth rate at low  $\Delta K$  relative to the same steel tested in argon at 400°C, 40 cpm (75). Later work showed that the apparent embrittling effect of lithium is increased at higher frequency, see Fig. 13 (77). At low frequencies, it was suggested, stress-assisted grain boundary penetration, leading to intergranular cracking, is enhanced, while at high frequencies a form of strain-rate induced transgranular LME occurs. Lithium could increase the crack growth rate relative to argon at  $\Delta K < 40$  ksi $\sqrt{\text{in}}$ , by weakening grain boundaries, while the improvement at high  $\Delta K$  could arise from screening of oxygen from crack tips, as observed for 316 SS in sodium, Fig. 14 (78). Sodium with a low impurity content (0.3 ppm C, 1 ppm O) has been shown to increase LCF life of 316 SS by three to four times, relative to air, while no effect of environment is noted in 304 SS (79). However, pre-exposure of 304 SS to sodium causes LCF life to be reduced at strain ranges above  $\Delta\epsilon_T = 0.8\%$ , with longer lives at strain ranges below this value. There is little effect, however, of pre-exposure of 316 SS to sodium. The difference in response of the two steels is attributed to greater depth of carbon penetration in 304 than in 316 under the pre-exposure conditions.

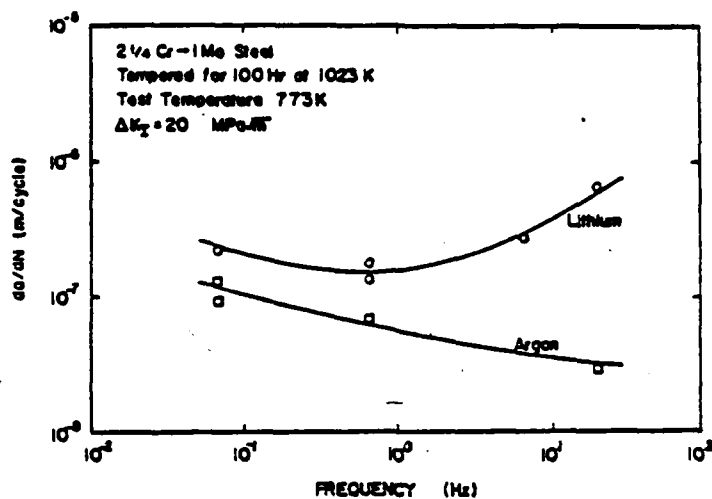


Fig. 13. Effect of frequency on crack growth rate,  $da/dN$ , for argon and lithium environments at  $773^\circ\text{K}$ ,  $\Delta K = 20 \text{ MPa m}^{1/2}$  (77).

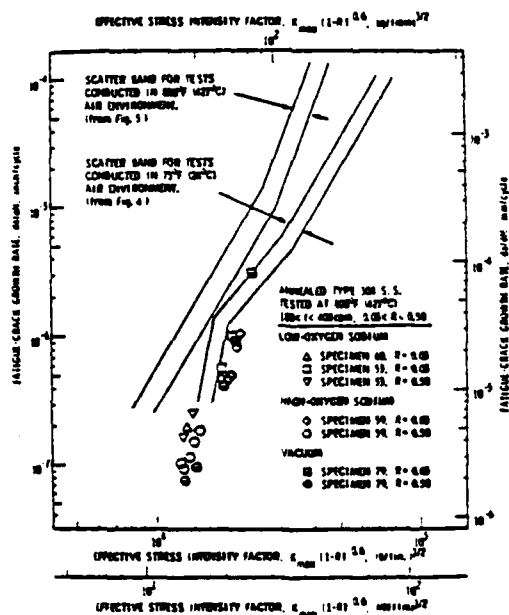


Fig. 14. Fatigue crack growth of 316 SS in sodium and in air at  $773^\circ\text{K}$  (78).

Metal-induced embrittlement encompasses an intriguing, complex set of phenomena which have not yet been satisfactorily explained. The metallurgical and environmental conditions favoring embrittlement are now well known, and several empirical techniques to rationalize or predict observed embrittlement have met with limited success. Our knowledge of possible transport mechanisms has been improved. The least success has been achieved in identifying an embrittlement mechanism which simultaneously can describe the interaction between embrittler and base metal, predict which combinations of environment and substrate will constitute embrittlement couples, and finally can explain the varied effects of metallurgical and test variables. As in the case of hydrogen embrittlement, there is reason to suspect that more than one mechanism is responsible for "classical" metal-induced embrittlement; for example, liquid metal embrittlement of amorphous metals is best explained by enhanced shear, liquid metal embrittlement of many crystalline metals can be explained by either enhanced shear or decohesion models, while solid-metal induced embrittlement and all forms of delayed failure phenomena may best be explained by a grain boundary penetration model.

Finally, degradation of structural alloys by alkali metals under monotonic and cyclic loading often, but not always, is controlled by the presence or absence of impurities. Experiments with nickel and palladium alloys as well as with amorphous alloys indicate that lithium, in particular, can have a devastating effect on mechanical properties even under conditions where impurity effects are minimal.

#### ACKNOWLEDGEMENTS

The author is grateful to Dr. S. Ashok and Mr. T. Slavin who have performed most of the experimental work on embrittlement of amorphous alloys; to Prof. Paul Gordon of Illinois Institute of Technology for providing a pre-publication copy of his manuscript, and to the Office of Naval Research for financial support under Contract No. N00014-79-C-0583.

#### REFERENCES

1. C. F. Old and P. Travena, Met. Science, 13:487 (1979).
2. J. C. Lynn, W. R. Warke and P. Gordon, Mat. Sci. Eng., 18:51 (1975).
3. E. D. Shchukin, Yu V. Goryunov, N. V. Pertsov and L. S. Bryukhanova, Sov. Mat. Sci., 14:341 (1978).
4. E. D. Shchukin, L. S. Bryukhanova, Z. M. Polukarova and N. V. Pertsov, Fiz. Khim. Mekh. Mater., 12, 40 (1976).
5. N. S. Stoloff in Environment-Sensitive Fracture of Engineering Materials, Z. A. Foroulis, Ed., AIME, New York, NY, 486 (1979).

6. G. Herbsleb and W. Schwenk, Werk. und Korrosion, 23:145 (1977).
7. F. A. Shunk, Ph.D. Thesis, Illinois Inst. of Technology (1976).
8. H. Nichols and W. Rostoker, Acta Met., 8:843 (1960).
9. M. C. Roth, G. C. Weatherly and W. A. Miller, Acta Met., 28: 841 (1980).
10. N. S. Stoloff and T. L. Johnston, Acta Met., 11:251 (1963).
11. N. S. Stoloff, R. G. Davies and T. L. Johnston in Environment-Sensitive Mechanical Behavior, Gordon and Breach, New York, 613 (1966).
12. A. H. Cottrell, Trans. Met. Soc. AIME, 212:192 (1958)
13. N. J. Petch in Fracture, Wiley, New York, 20 (1959).
14. A. S. Tetelman and A. J. McEvily, Jr., Fracture of Structural Materials, Wiley, New York, 268 (1967).
15. K. L. Johnson, N. N. Breyer and J. W. Dally, Proc. Conf. on Environmental Degradation of Engineering Materials, Blacksburg, VA, 91 (1977).
16. W. M. Robertson, Met. Trans., 1: 2607 (1970).
17. W. Rostoker, J. M. McCaughey and H. Markus, in Embrittlement by Liquid Metals, Reinhold, New York (1960).
18. C. M. Preece and A. R. C. Westwood, Trans. ASM, 62:418 (1969).
19. A. S. Tetelman and S. Kunz, in Proc. Int. Conf. on Stress Corrosion Cracking and Hydrogen Embrittlement of Iron-Base Alloys, Unieux-Firminy, 359 (1977).
20. V. V. Popovich and I. G. Dmukhouskaya, Sov. Mat. Sci., 14:365 (1978).
21. A. R. C. Westwood and M. Kamdar, Phil. Mag., 8:787 (1963).
22. P. Gordon, Met. Trans. A, 9A:267 (1978).
23. N. A. Gjostein, in Diffusion, American Soc. for Metals, Metals Park, OH, 241 (1973).
24. M. J. Kelley and N. S. Stoloff, Met. Trans. A, 6A: 159 (1975).
25. N. Engel, Powder Met. Bull., 7:8 (1954).
26. L. Brewer, in High Strength Materials, V. F. Zackay, Ed., Wiley, New York, 12 (1975).
27. R. M. German, in The Metal Science of Stainless Steels, E. W. Collings and H. W. King, Eds., 41, AIME, New York, (1978).
28. J. H. Hildebrand and R. L. Scott, Solubility of Non-Electrolytes, 3rd Ed., Prentice Hall, Englewood Cliffs, NJ (1950).
29. A. A. Griffith, Trans. Roy. Soc. Lond., 221:163 (1920).
30. E. Orowan, Welding J., 34:1575 (1955).
31. H. K. Birnbaum, in Environment-Sensitive Fracture of Engineering Materials, Z. A. Zoroulis, Ed., AIME, New York, NY, 326 (1979).
32. M. L. Jokl, V. Vitek and C. J. McMahon, Jr., Acta Met., 28: 1479 (1980).
33. J. J. Gilman, Plasticity - Proc. Sec. Symp. on Naval Structural Mechanics, 43, Pergamon Press, New York (1960).
34. C. F. Old, in Fracture 1977 Proc. ICF4, D. M. R. Taplin, Ed., Waterloo, Canada, 2:331 (1977).
35. M. H. Kamdar, Prog. Mat. Sci., 15:289 (1973).

36. M. G. Nicholas and C. F. Old, J. Mat. Sci., 14:1 (1979).
37. C. F. Old and P. Travena, Met. Sci., 13:591 (1979).
38. M. I. Chaevskii, Sov. Mat. Sci., 1:433 (1965).
39. C. F. Old and P. Travena, Proc. Third Int. Conf. on Mechanical Behavior of Materials 2, Pergamon Press, Oxford, 397 (1980).
40. G. M. Scamans and C. D. S. Tuck, Sec. Int. Cong. on Hydrogen in Metals, Paris, 1977, Pergamon Press, paper 4A-11.
41. J. J. Gilman, Discussion to ref. 19, p. 375.
42. N. Toropovskaya, Sov. Mat. Sci., 6:324 (1970).
43. R. A. Oriani, in Proc. Int. Conf. on Stress Corrosion Cracking and Hydrogen Embrittlement of Iron-Base Alloys, Unieux-Firminy, 351 (1977).
44. F. A. Shunk and W. R. Warke, Scripta Met., 519 (1974).
45. P. Gordon, Illinois Inst. of Technology, unpublished (1981).
46. Y. Iwata, Y. Asayama and A. Sakamoto, J. Jap. Inst. Met., 21: 77 (1967).
47. J. V. Rinnovatore, J. D. Corrie and H. Markus, Trans. ASM, 59: 665 (1966).
48. L. S. Bryakhanova, I. A. Andreeva and V. I. Likhman, Sov. Phys. Solid State, 3:2025 (1962).
49. C. M. Preece and A. R. C. Westwood, in Fracture, Proc. Sec. Int. Conf. on Fracture, Chapman and Hall, London, 439 (1969).
50. E. A. Clark, R. Yeske and H. K. Birnbaum, Met. Trans. A, 11A: 1903 (1980).
51. S. P. Lynch, Scripta Met., 13:1051 (1977).
52. S. P. Lynch, "The Mechanism of Liquid Metal Embrittlement - Crack Growth in Aluminum Single Crystals, A.R.L. Mat. Report 102, Aeronautical Res. Labs, Melbourne, Australia (1977).
53. S. P. Lynch, Acta Met., 29:325 (1981).
54. S. P. Lynch and N. E. Ryan, Proc. Sec. Int. Cong. on Hydrogen in Metals, paper 3D12, Pergamon, Oxford (1977).
55. S. P. Lynch, in Fatigue Mechanisms, ASTM STP675, Amer. Soc. for Test. and Materials, Philadelphia, PA, 174 (1979).
56. M. A. Krishtal, Sov. Phys. Dokl., 15:614 (1970).
57. H. Matsui, H. Kimura and S. Moriya, Proc. Fourth Int. Conf. on Strength of Metals and Alloys, 291 (1976).
58. H. Matsui, H. Kimura and S. Moriya, Mat. Sci. Eng., 40:207 (1979).
59. R. A. Oriani and P. H. Josephic, Met. Trans. A, 11A, 1809 (1980).
60. J. A. Clum, Scripta Met., 9:51 (1975).
61. R. J. H. Wanhill, Corrosion, 29:435 (1973).
62. W. R. Goggin and J. W. Moberly, Trans. ASM, 59:315 (1966).
63. N. A. Tiner, Trans. Met. Soc. AIME, 221:261 (1961).
64. S. Ashok, N. S. Stoloff, M. E. Glicksman and T. P. Slavin, Scripta Met., 15:331 (1981).
65. E. E. Glikman and Yu. V. Goryunov, Fiz. Khim. Mekh. Mater., 14:20 (1978).

66. E. E. Glikman, Yu. V. Goryunov, V. M. Demin and K. Yu. Sarychev, Izv. Vyssh. Uchebn. Zaved. Fiz., 15 (1976).
67. S. K. Marya and G. Wyon, Scripta Met., 9:1009 (1975).
68. L. S. Soldachenkova, Sov. Mat. Sci., 11:251 (1975).
69. H. Nelson and D. P. Williams, Met. Trans., 1:63 (1970).
70. I. M. Bernstein, Mat. Sci. Eng., 6:1 (1970).
71. S. P. Lynch, Proc. Fourth Int. Conf. on Fracture, D. M. R. Taplin, Ed., 2, Waterloo, Canada, 859 (1977).
72. N. N. Breyer and K. L. Johnson, J. Test. and Eval. 2: 471 (1974).
73. K. Yoshino and C. J. McMahon, Jr., Met. Trans. A, 5A: 363 (1974).
74. N. M. Parikh, in Environment-Sensitive Mechanical Behavior, A. R. C. Westwood and N. S. Stoloff, Eds., Gordon and Breach, New York, 563 (1966).
75. D. L. Hammon, S. K. DeWeese, D. K. Matlock and D. L. Olson, Closed Loop, 9:3 (1979).
76. S. Ashok and N. S. Stoloff, unpublished.
77. R. E. Spencey, S. K. DeWeese, D. K. Matlok and D. L. Olson, Met. Trans. A, 11A:1758 (1980).
78. L. A. James and R. L. Knecht, Met. Trans. A, 6A:109 (1975).
79. D. L. Smith and G. J. Zeman, Closed Loop, 9:12 (1979).

Unclassified

SECURITY CLASSIFICATION OF THIS PAGE (When Data Entered)

REPORT DOCUMENTATION PAGE		READ INSTRUCTIONS BEFORE COMPLETING FORM	
1. REPORT NUMBER 3	2. GOVT ACCESSION NO. AD A103	3. RECIPIENT'S CATALOG NUMBER 048	
4. TITLE (and Subtitle)  Liquid and Solid Metal Embrittlement		5. TYPE OF REPORT & PERIOD COVERED  Technical	
		6. PERFORMING ORG. REPORT NUMBER	
7. AUTHOR(s)  N.S. Stoloff		8. CONTACT OR GRANT NUMBER(s)  N00014 - 79C9583	
9. PERFORMING ORGANIZATION NAME AND ADDRESS Materials Engineering Department Rensselaer Polytechnic Institute Troy, New York 12181		10. PROGRAM ELEMENT, PROJECT, TASK AREA & WORK UNIT NUMBERS	
11. CONTROLLING OFFICE NAME AND ADDRESS Office of Naval Research Arlington, Virginia		12. REPORT DATE September 5, 1981	
		13. NUMBER OF PAGES 29	
14. MONITORING AGENCY NAME & ADDRESS (if different from Controlling Office) Office of Naval Research Resident Representative 715 Broadway Fifth Floor New York, NY 10003		15. SECURITY CLASS. (of this report)  Unclassified	
		15a. DECLASSIFICATION/DOWNGRADING SCHEDULE	
16. DISTRIBUTION STATEMENT (of this Report)  Reproduction in whole or in part is permitted for any purpose of the United States Government. Distribution of this document is unlimited.			
17. DISTRIBUTION STATEMENT (of the abstract entered in Block 20, if different from Report)			
18. SUPPLEMENTARY NOTES			
19. KEY WORDS (Continue on reverse side if necessary and identify by block number) aluminum                      iron                                      strain rate amorphous                      liquid decohesion                      metal embrittlement                      nickel fracture                              shear			
20. ABSTRACT (Continue on reverse side if necessary and identify by block number) The recent literature on embrittlement induced by solid or liquid metal environments is critically reviewed. Evidence in support of an enhanced shear model of embrittlement is provided for amorphous metals, while decohe- sion is shown to be a viable concept for crystalline metals. The usefulness of the concept of specificity of embrittlement is questioned on the basis of evidence for new embrittlement couples as the range of experimental conditions is varied. In particular, strain rate and temperature are shown to have			

DD FORM 1473  
1 JAN 73

EDITION OF 1 NOV 68 IS OBSOLETE  
S/N 0102-LF-014-6601

Unclassified

SECURITY CLASSIFICATION OF THIS PAGE (When Data Entered)



Unclassified

SECURITY CLASSIFICATION OF THIS PAGE (When Data Entered)

extremely important effects on the degree of embrittlement.

Unclassified

SECURITY CLASSIFICATION OF THIS PAGE (When Data Entered)

